Hunziker, W., Siebert, P. D., King, M. W., Stucki, P., Dugaicyk, A., & Norman, A. W. (1983) *Proc. Natl. Acad. Sci. U.S.A. 80*, 4228-4232.
Kilhoffer, M. C., Haiech, J., & Demaille, J. G. (1983) *Mol. Cell. Biochem. 51*, 33-54.
King, M. W., & Norman, A. W. (1986) *Arch. Biochem. Biophys. 248*, 612-619.
Kretsinger, R. H. (1976) *Annu. Rev. Biochem. 45*, 239-266.
Laemmli, U. K. (1970) *Nature (London) 227*, 680-685.
Mangelsdorf, D. J., Pike, J. W., & Haussler, M. R. (1987) *Proc. Natl. Acad. Sci. U.S.A. 84*, 354-358.
Maniatis, T., Fritsch, E., & Sambrook, J. (1982) *Molecular Cloning: A Laboratory Manual*, Cold Spring Harbor Laboratory, Cold Spring Harbor, NY.
McDonnell, D. P., Mangelsdorf, D. J., Pike, J. W., Haussler, M. R., & O'Malley, B. W. (1987) *Science (Washington, D.C.) 235*, 1214-1217.
McNutt, K. W., & Haussler, M. R. (1973) *J. Nutr. 103*, 681-689.
Means, A. R., Tash, J. S., & Chafouleas, J. G. (1982) *Physiol. Rev. 62*, 1-38.
Nojima, H., & Sokabe, H. (1986) *J. Mol. Biol. 190*, 391-400.
Nojima, H., Kishi, K., & Sokabe, H. (1986) *J. Hypertens. 4 (Suppl. 3)*, S275-S277.
Ouchterlony, O. (1962) *Prog. Allergy 6*, 30-75.
Pike, J. W., Sleator, N. M., & Haussler, M. R. (1987) *J. Biol. Chem. 262*, 1305-1311.
Plancke, Y. D., & Lazarides, E. (1983) *Mol. Cell. Biol. 3*, 1412-1420.
Rasmussen, H. (1986) *N. Engl. J. Med. 314*, 1094-1101.
Sanger, F., Nicklen, S., & Coulson, A. R. (1977) *Proc. Natl. Acad. Sci. U.S.A. 74*, 5463-5467.
Simmen, R. C. M., Tanaka, T., Ts'ui, K. F., Putkey, J. A., Scott, M. J., Lai, E. C., & Means, A. R. (1985) *J. Biol. Chem. 260*, 907-912.
Southern, E. M. (1975) *J. Mol. Biol. 98*, 503-517.
Theofan, G., Nguyen, A. P., & Norman, A. W. (1986) *J. Biol. Chem. 261*, 16943-16947.
Thomas, P. (1980) *Proc. Natl. Acad. Sci. U.S.A. 77*, 5201-5205.
Towbin, H., Staehelin, T., & Gordon, J. (1979) *Proc. Natl. Acad. Sci. U.S.A. 76*, 4350-4354.
Ullrich, A., Shine, J., Chirgwin, J., Pictet, R., Tischer, E., Rutter, W. J., & Goodman, H. M. (1977) *Science (Washington, D.C.) 196*, 1313-1319.
Wasserman, R. H., & Taylor, A. N. (1966) *Science (Washington, D.C.) 152*, 791-793.
Wasserman, R. H., Corradino, R. A., & Taylor, A. N. (1968) *J. Biol. Chem. 243*, 3978-3986.
Wilson, P. W., Harding, M., & Lawson, D. E. M. (1985) *Nucleic Acids Res. 13*, 8867-8881.
Yamamoto, K. R. (1985) *Annu. Rev. Genet. 19*, 209-252.
Young, R. A., & Davis, R. W. (1983) *Proc. Natl. Acad. Sci. U.S.A. 80*, 1194-1198.

Phase-Resolved Spectral Measurements with Several Two Tryptophan Containing Proteins†

Maurice R. Eftink,*,‡ Zygmunt Wasylewski,§ and Camillo A. Ghiron‖

Department of Chemistry, University of Mississippi, University, Mississippi 38677, Department of Biochemistry, Jagellonian University, Krakow, Poland, and Department of Biochemistry, University of Missouri, Columbia, Missouri 65201

Received June 12, 1987; Revised Manuscript Received August 12, 1987

ABSTRACT: We have used frequency domain fluorescence techniques to resolve the component emission spectra for several two tryptophan containing proteins (e.g., horse liver alcohol dehydrogenase, sperm whale apomyoglobin, yeast 3-phosphoglycerate kinase, apoazurin from *Alcaligenes denitricans*). We have first performed multifrequency phase/modulation measurements and have found the fluorescence of each of these proteins to be described by a double exponential. Then, using phase-sensitive detection and the algorithm of Gratton and Jameson [Gratton, E., & Jameson, D. M. (1985) *Anal. Chem. 57*, 1694-1697], we have determined the emission spectrum associated with each decay time for these proteins. We have compared these phase-resolved spectra with the fractional contributions of the component fluorophores determined by selective solute quenching experiments. Reasonably good agreement is seen in most cases, which argues that the individual Trp residues emit independently. In the case of apoazurin, however, a negative amplitude is seen for the phase-resolved spectrum of the short-lifetime component. This pattern is consistent with the occurrence of energy transfer from the internal Trp residue to the surface Trp of this protein. We also present multifrequency lifetime measurements, phase-resolved spectra, and solute quenching data for a few protein–ligand complexes, to illustrate the utility of this approach for the study of changes in the fluorescence of proteins.

The fluorescence emission of most proteins and other biochemical assemblies is heterogeneous, due to ground-state hetereogeneity or excited-state reactions (Beechem & Brand, 1985; Longworth, 1983). For example, most proteins possess more than one Trp residue, and since the fluorescence properties of the indole nucleus are environment dependent, the experimentally measured fluorescence spectra, quantum yields, lifetimes, or anisotropies will be a composite or average over the individual components. Such heterogeneity makes the interpretation of fluorescence data much more difficult. It is often desirable to be able to resolve the fluorescence of a system into its components. For example, if one can resolve and assign the fluorescence signals of individual Trp residues

† This research was supported by NSF Grant DMB 85-11569 to M.R.E.
‡ University of Mississippi.
§ Jagellonian University.
‖ University of Missouri.

0006-2960/87/0426-8338$01.50/0

in proteins, then these residues become valuable, intrinsic probes for monitoring changes in the protein.

To resolve the fluorescence of a heterogeneous system, one can take advantage of differences in spectral position (Weber, 1961), fluorescence lifetime (Ross et al., 1981; Grinvald & Steinberg, 1976; Brochon et al., 1974), anisotropy (Anderson et al., 1970), or accessibility to quenchers (Lehrer, 1971; Eftink & Ghiron, 1976), of the different components. Since Trp residues in proteins have a modestly large range of intrinsic lifetimes (Beechem & Brand, 1985), a powerful method involves the determination of decay-associated spectra (DAS),[1] that is, the emission spectra associated with particular decay times in a heterogeneously emitting system. Knutson et al. (1982) have developed the use of this strategy with time domain (i.e., pulse, single-photon-counting) measurements, to resolve the fluorescence of the two Trp residues of the protein liver alcohol dehydrogenase.

Recently, analogous frequency domain methods, involving either electronic or computational procedures, have been developed for resolving heterogeneously emitting systems. Using a phase-sensitive detection system, Lakowicz and Cherek (1981) demonstrated the ability to resolve the subspectra of indole mixtures and the subspectra of Tyr and Trp residues in a denatured protein. Gratton and Jameson (1985) developed a similar software approach for obtaining such phase-resolved spectra (PRS) of mixtures from frequency domain data. With either the hardware or software method, only a single modulation frequency is required, but as with time-resolved methods, a significant difference between the decay times of components is required to achieve resolution. Independent determination of the decay times of components is generally required [or alternatively, independent knowledge of the subspectra is required to resolve the component decay times (Keating-Nakamoto et al., 1986)].

Below we will report some of the first PRS measurements with native proteins. This method, along with the analogous DAS method involving time domain measurements, should become a valuable tool for studying protein fluorescence. Here, we will report studies with a number of two tryptophan containing proteins, and we will show cases in which a clean resolution of the spectra of the individual Trp residues is possible. We also consider the complications that may arise when excited-state reactions occur, such as energy transfer between Trp residues. We will demonstrate that in favorable cases (e.g., in a two-Trp apoazurin) PRS can indicate the existence of such homotransfer. We also will illustrate the usefulness of comparing PRS with steady-state solute quenching data.

Materials and Methods

Materials. Azurin from *Alcaligenes denitricans* (Ade) was a generous gift from Dr. G. E. Norris, Massey University, Palmerston North, New Zealand. Apoazurin was prepared by the method of Blaszak et al. (1983). Ribulose-5-phosphate kinase (RPK) from spinach was a generous gift from Drs. M. A. Porter and F. C. Hartman, Oak Ridge National Laboratory. Horse liver alcohol dehydrogenase (LADH) was obtained from Cal-Biochemical (San Diego, CA) as a crystalline suspension in 20% ethanol. The sample was dialyzed to remove ethanol prior to being studied. 3-Phosphoglycerate kinase (PGK) from yeast was obtained as a crystalline suspension from Sigma Chemical Co. (St. Louis, MO) and was also dialyzed before use. Sperm whale apomyoglobin was prepared from the holoprotein (Sigma) as described by Theorell and Åkeson (1955). Metalloprotease from *Staphylococcus aureus* strain V8/10B was isolated following the procedure of Drapelu (1978), with the small modification described previously (Wasylewski et al., 1986). Bovine β-lactoglobulin was obtained from Sigma Chemical Co.

The lithium salt of β-NAD^+ was obtained from Cal-Biochem; 3-phosphoglycerate, ATP, and EDTA were obtained from Sigma Chemical Co. Potassium iodide was obtained from Aldrich Chemical Co. Indole and 3-methylindole were sublimed before use. Acrylamide was recrystallized from ethyl acetate.

Methods. An SLM (Champaign, IL) 4800 phase/modulation fluorometer, equipped with a Pockels cell, frequency synthesizers, and a 150-W xenon lamp from ISS (Champaign, IL), was used to measure multifrequency (10–200 MHz) phase and modulation lifetimes. These lifetimes were measured with respect to *p*-terphenyl as a reference compound. Measurements were made at 20 °C. An excitation interference filter, centered at 290 nm, was used, and the emission was observed through a Corning 7/60 band-pass filter. The data were analyzed by nonlinear least squares to obtain the best single-exponential and double-exponential fits (Gratton et al., 1984). For each of the proteins studied here a double-exponential fit was found to be superior.

Steady-state fluorescence quenching experiments were performed with the above instrument, but with a monochromater in the excitation path. Quenching data were fitted to the Stern–Volmer equation (eq 1) for a heterogeneous system, using the nonlinear least-squares procedure of Stryjewski and Wasylewski (1986). In this equation F and F_0

$$\frac{F}{F_0} = \sum_{i=1}^{n} \frac{f_i}{(1 + K_i[Q])\exp(V_i[Q])} \tag{1}$$

are the fluorescence intensities in the presence and absence of quencher Q, f_i is the fractional intensity of component i at the emission and excitation wavelengths employed, K_i is the dynamic Stern–Volmer quenching constant of component i, and V_i is the static quenching constant of component i.

Phase-resolved spectra were performed with an SLM 4800 phase fluorometer. This instrument uses a Debye–Sears modulator tank, and a modulation frequency of 30 MHz was employed. To improve the signal, a 350-W xenon lamp and a 290-nm interference filter were used for excitation. The emission was measured through a monochromater (16-nm slits) and detected with an EMI photomultiplier. Phase angles and relative modulations were determined at 2-nm intervals from about 300 to above 400 nm. A typical, manual scan took about 20 min. Software from ISS was then used to resolve the emission spectra of the components. A glycogen scattering solution was used as a reference. We checked the reference phase angle immediately before and after the sample scan to ensure that the instrument did not drift significantly during the course of the measurements.

As explained by Gratton and Jameson (1985), the ratio of the fractional intensities of two components can be determined by measurements of the apparent phase lifetime τ_p of a sample at a single modulation frequency ω, provided that τ_1 and τ_2 are known:

$$\frac{f_1}{f_2} = \frac{(\tau_2 - \tau_p)(1 + \omega^2\tau_1^2)}{(\tau_p - \tau_1)(1 + \omega^2\tau_2^2)} \tag{2}$$

[1] Abbreviations: Ade, *Alcaligenes denitricans*; bicine, *N,N*-bis(2-hydroxyethyl)glycine; DAS, decay-associated spectra; LADH, horse liver alcohol dehydrogenase; NAD^+, β-nicotinamide adenine dinucleotide; Pae, *Pseudomonas aeruginosa*; PGK, yeast 3-phosphoglycerate kinase; PRS, phase-resolved spectra; RPK, spinach ribulose-5-phosphate kinase; TFE, trifluoroethanol.

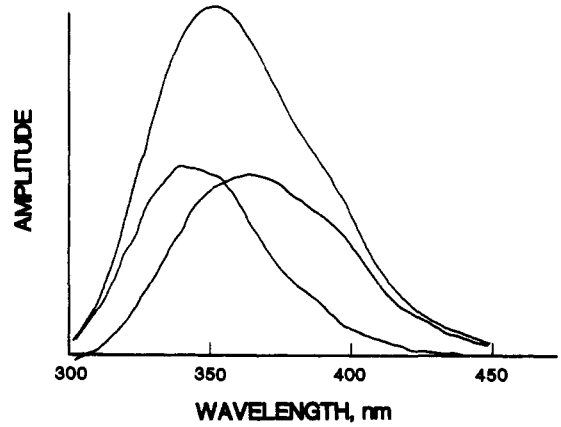

FIGURE 1: Phase-resolved spectra for a mixture of indole and 3-methylindole in water at 20 °C. The top curve is the total steady-state emission spectrum. The blue and red spectra correspond to the components with τ_1 = 4.4 ns and τ_2 = 8.5 ns. The mixture was prepared to have approximately equal emission of the components at 350 nm.

Table I: Fluorescence Decay Parameters for Selected Two Tryptophan Containing Proteins[a]

protein	τ_1 (ns)	f_1	τ_2 (ns)	f_2
apoazurin (Ade) (280 nm)[b]	0.79	0.107	3.52	0.893
apoazurin (Ade)[b]	1.32	0.119	3.56	0.881
apomyoglobin[c]	1.31	0.539	4.08	0.461
β-lactoglobulin[c]	1.13	0.766	2.79	0.234
LADH[c]	3.38	0.439	6.74	0.561
metalloprotease[d]	1.17	0.50	5.08	0.50
PGK[e]	0.39	0.728	3.49	0.272
RPK[f]	1.83	0.426	6.39	0.574

[a] Excitation at 290 nm, except as indicated for apoazurin (Ade). Temperature, 20 °C. The f_i values refer to the fractional contribution for emission observed through a band-pass filter having maximum transmission at 350 nm and a half-width of 50 nm. [b] In 0.05 M sodium acetate buffer, pH 5.0. [c] In 0.02 M sodium phosphate, pH 7.5. [d] In 0.05 M Tris-HCl buffer, pH 9.0, containing 10 mM $CaCl_2$. [e] In 0.05 M Tris-HCl buffer, pH 7.2, with 0.1 M NaCl. [f] In 0.01 M bicine buffer, pH 8.0, with 0.1 mM EDTA and 5% glycerol.

By simultaneous measurement of the steady-state intensity spectrum, eq 2 allows phase-resolved subspectra for the two components to be calculated. A similar expression exists for apparent modulation lifetimes, but our experience is that τ_p measurements with a Debye–Sears modulation tank are more stable than measurements of τ_m, the apparent modulation lifetime.

RESULTS

Indole Mixtures. In Figure 1 is shown the emission spectrum of a mixture of indole and 3-methylindole in water. From previous studies we know that the fluorescence decay of these individual compounds is a single exponential and that the fluorescence lifetimes are 4.4 and 8.5 ns for indole and 3-methylindole, respectively, at 20 °C. Using these lifetimes, we resolve the composite spectrum into two components as shown in Figure 1. The spectrum of the 4.4-ns component has a maximum at 340–345 nm, and the spectrum of the 8.5-ns component has a maximum at 365 nm. These λ_{max} values are the same as those found for pure aqueous solutions of indole and 3-methylindole.

Proteins—Fluorescence Lifetime Measurements. For the six proteins listed in Table I, we have performed multifrequency phase and modulation measurements. For each protein a fit to a single-exponential decay is unsatisfactory; the best double-exponential fits are given. In Figure 2 are shown typical multifrequency phase and modulation data and double-exponential fits for the proteins apomyoglobin and apoazurin (Ade).

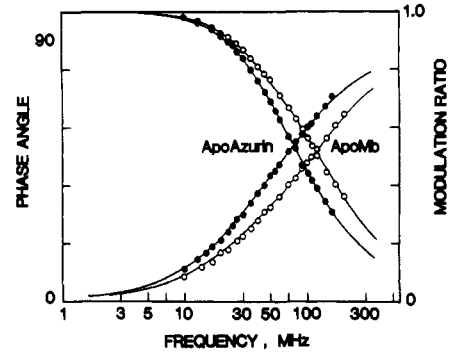

FIGURE 2: Multifrequency phase and modulation data for apomyoglobin (sperm whale) and apoazurin (Ade). Conditions: excitation at 290 nm, 20 °C, buffers as indicated in Table I. Two-component fits are given in Table I.

For some of these proteins there are literature fluorescence lifetime values with which we can compare our values. Much work has been done with LADH, and it is well established that one of its Trp residues, Trp-314, has a lifetime of 3–4 ns and that the other Trp residue, Trp-315, has a lifetime of about 7 ns (Ross et al., 1981; Knutson et al., 1982; Eftink & Hagaman, 1986). Our results are consistent with these values, although our τ values run on the low side for each residue. For apomyoglobin, Janes et al. (1987) have reported a triple-exponential fit to pulse–decay data (297-nm excitation) with τ_1 = 0.2 ns, τ_2 = 1.35 ns, τ_3 = 3.9 ns, f_1 = 0.035, f_2 = 0.295, and f_3 = 0.67. Since their τ_1 component has such a small fractional contribution, our two-component fit is actually in good agreement with the three-component fit of Janes et al. Also, steady-state fluorescence studies with apomyoglobin indicate that the two Trp residues of this protein have different degrees of solvent exposure (Irace et al., 1981; Anderson et al., 1970). For PGK, Privat et al. (1980) have previously shown that the decay of this protein can best be described as a triple exponential. As we have presented elsewhere (Wasylewski & Eftink, 1987a), our phase domain data is not of high enough quality to attempt a three-component fit, but the τ_2 value we report for PGK is equal to the average of the two longer lifetimes reported by Privat et al. Thus our two-component fit is in crude agreement with the mentioned work. For apoazurin Ade, Petrich et al. (1987) report a double-exponential fit of τ_1 = 1.28 ns and τ_2 = 3.55 ns (292-nm excitation). Our decay times for this protein are very similar, when one considers excitation at 290 nm (at 280 nm the τ_1 value may be shortened due to energy transfer—see below). The other proteins have not been significantly studied from a fluorescence point of view. We have also measured the fluorescence decay of the single Trp containing apoazurin from *Pseudomonas aeruginosa* (Pae). This protein has been found by others to have a monoexponential decay (Szabo et al., 1983; Petrich et al., 1987). We find more then 98% of the intensity to be associated with a lifetime of 4.0 ns. Thus, with our phase fluorometer we concur that the fluorescence of apoazurin Pae is essentially a single exponential.

Proteins—Phase-Resolved Spectra. Using the τ_1 and τ_2 values in Table I for the various proteins, we obtained frequency domain emission spectra and calculated from this data the PRS of each lifetime. In Figure 3 are shown PRS of various proteins. A clean resolution of the components is possible in each case. Perhaps it is a coincidence, but the short-lifetime component is found to be bluer than the long-lifetime component for each protein. For most proteins (except

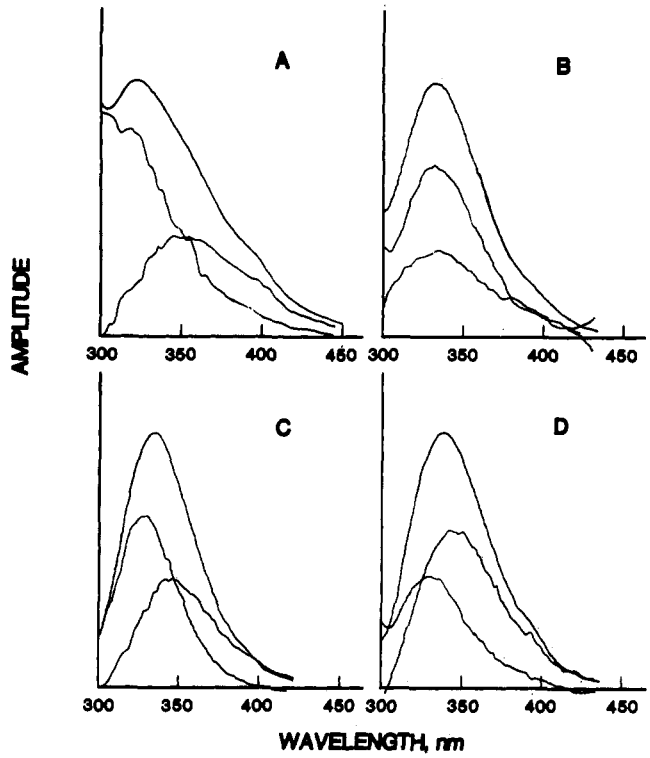

FIGURE 3: Phase-resolved spectra for several two-tryptophan proteins: (A) metalloprotease, (B) apomyoglobin, (C), PGK, and (D) RPK. See Table I for the lifetimes for the components and the conditions. In each case, the short-lifetime component is the bluer spectrum. The top spectrum in each case is the steady-state emission spectrum.

Table II: Phase-Resolved Spectra for Selected Two Tryptophan Containing Proteins[a]

protein	$\lambda_{max,1}$ (nm)	f_1	$\lambda_{max,2}$ (nm)	f_2
apoazurin (Ade)	312	0.20	346	0.80
apomyoglobin	330	0.53	347	0.47
β-lactoglobulin	335	0.67	340	0.33
LADH	324	0.39	340	0.61
metalloprotease	318	0.58	355	0.42
PGK	329	0.64	339	0.36
RPK	325	0.40	345	0.60

[a] Conditions given in Table I. The f_i values refer to the integrated relative intensities corresponding to the PRS for the individual lifetimes.

apoazurin at 280-nm excitation, see below), the shape of each component spectrum is reasonable, in that there are no abnormally skewed spectra and the spectra do not dip below the x axis. In Table II we give the λ_{max} of each component (subscript 1 refers to the short-lifetime component and subscript 2 refers to the long-lifetime component) and the integrated fractional contribution of each.

PRS measurements with apoazurin from *A. denitricans* are shown in Figure 4. The left and right panels are for excitation wavelengths of 280 and 290 nm, respectively. As can be seen, the maxima of the short-lifetime component ($\lambda_{max} \approx 312$ nm) and the long-lifetime component ($\lambda_{max} \approx 346$ nm) are widely separated. The short-lifetime component appears to drop below the x axis between 330 and 350 nm. The negative amplitude of this component is much more pronounced with 280-nm excitation than with 290-nm excitation. As will be discussed below, this pattern is consistent with energy transfer between the blue and red Trp residues of apoazurin.

Solute Quenching Studies. Potassium iodide or acrylamide was used as a solute quencher with these two tryptophan containing proteins. For each of the proteins in Table III we found the Stern–Volmer plots to be downward curving, which

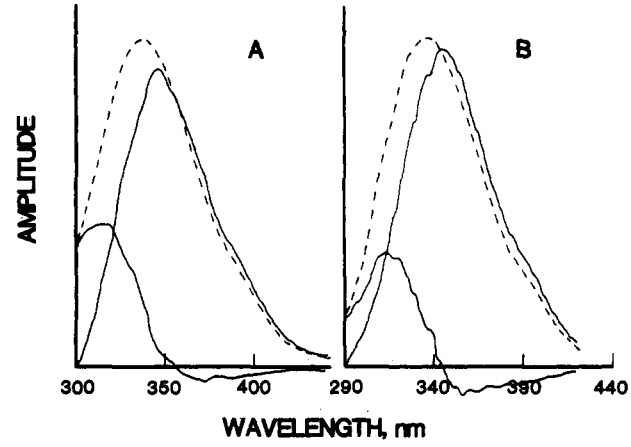

FIGURE 4: Phase-resolved spectra for apoazurin (Ade): excitation at 290 (A) and 280 nm (B). The lifetimes for the components are $\tau_1 = 0.79$ ns and $\tau_2 = 3.52$ ns at 280-nm excitation and $\tau_1 = 1.32$ ns and $\tau_2 = 3.56$ ns at 290-nm excitation. The shorter lifetime component is the bluer emitting spectrum. Note the different wavelength scales.

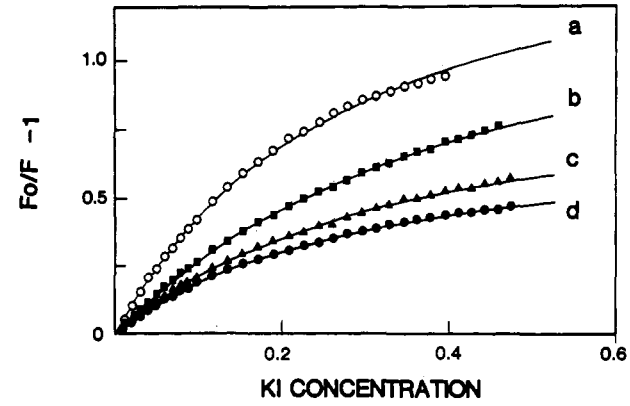

FIGURE 5: Stern–Volmer plots for iodide quenching of selected two tryptophan containing proteins at 20 °C, when excited at 290 nm: (a) LADH·NAD^+·TFE ternary complex; (b) apomyoglobin; (c) metalloprotease; and (d) LADH. Conditions and fitting parameters are given in Table III.

Table III: Stern–Volmer Quenching Constants for Acrylamide and Iodide Quenching of Fluorescence of Selective Two Tryptophan Containing Proteins[a]

quencher and protein	f_1	K_1 (M^{-1})	f_2	K_2 (M^{-1})
acrylamide				
apoazurin (Ade)	0.23	0.46	0.77	5.10
RPK	0.55	0.73	0.45	6.38
iodide				
apomyoglobin	0.40	0	0.60	5.38
LADH	0.45	0	0.55	4.60
metalloprotease	0.50	0	0.50	5.42

[a] Excitation at 295 nm in all cases. Conditions given in Table I.

indicates that the quencher is able to selectively quench the emission of the more accessible fluorescing components. Figure 5 shows Stern–Volmer plots for apomyoglobin, LADH, the LADH ternary complex, and metalloprotease. Equation 1 was fitted to these data by nonlinear least squares (Stryjewski & Wasylewski, 1986); the fitting parameters are shown in Table III. For the above-mentioned four proteins, the iodide quenching data are well described by a two-component model, with one component (fraction f_1) being completely inaccessible ($K_1 = 0$) to iodide. (Iodide was found to not quench the fluorescence of the proteins PGK and β-lactoglobulin.) These experiments were performed with a broad-band emission filter (same as used for the lifetime studies), and the fractional intensities should be similar to the integrated values obtained

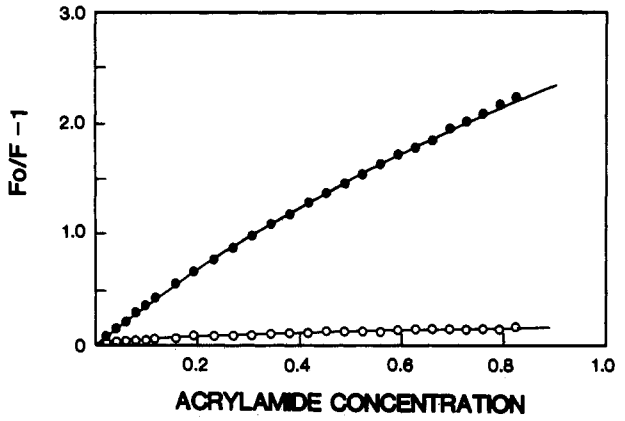

FIGURE 6: Stern–Volmer plots for acrylamide quenching of apoazurin Ade (●) and apoazurin Pae (○). Conditions and fitting parameters are given in Table III.

from the PRS (assuming that there are two independent emitting centers—see below). As can be seen, the f_2 values obtained by iodide quenching do agree reasonably well with the fractional intensities found in both the lifetime and PRS studies.

Acrylamide quenching of the fluorescence of apoazurin Ade is shown in Figure 6. A clear downward curvature is seen, and a fit of eq 2 shows that the minor component is less accessible, but not completely inaccessible (K_1 = 0.46 M^{-1}), to acrylamide. This K_1 value obviously characterizes the quenching of the internal Trp-48 of apoazurin Ade. With the lifetime of 1.32 ns found for this residue, its kinetic exposure to acrylamide is given by a quenching rate constant k_q equal to about 0.35 × 10^9 M^{-1} s^{-1}. Such a k_q value is similar in magnitude to that for the acrylamide quenching of other internal Trp residues in proteins such as ribonuclease T_1 and cod parvalbumin (Eftink & Hagaman, 1985; Eftink & Ghiron, 1987). The surface Trp residue, Trp-118, on the other hand, is much more exposed to the solute quencher (k_q = 1.4 × 10^9 M^{-1} s^{-1}).

For comparison, we also show in Figure 6 the acrylamide quenching of the single, internal Trp-48 of the apoazurin from *P. aeruginosa* (Pae). The quenching data for this protein are similar to those previously published by Mallinson et al. (1981); the effective k_q value is only about 0.05 × 10^9 M^{-1} s^{-1}, one of the lowest values found for residues in proteins. The slight difference between the k_q values for the internal Trp in the two apoazurins must reflect a subtle difference in the structure and/or location of this residue between the two proteins.

Proteins—Ligand Binding Studies. We have used the PRS method to investigate changes in the fluorescence of proteins upon the binding of specific ligands. For example, Figure 7 shows PRS of LADH and its ternary complex with NAD^+ and trifluoroethanol. Likewise, we have studied the effect of the ligands ATP and 3-phosphoglycerate on the fluorescence of PGK (Wasylewski & Eftink, 1987a) and the effect of removal of calcium ions on the fluorescence of metalloprotease (Wasylewski & Eftink, 1987b). In Table IV we list lifetime, PRS, and iodide quenching studies for these ligand binding systems. Some dramatic and selective fluorescence changes can be seen. For example, the binding of 3-phosphoglycerate causes a selective red shift in the fluorescence of the short-lifetime component of PGK. The removal of Ca^{2+} results in a 20-nm red shift in the short-lifetime component of metalloprotease. The binding of NAD^+ and trifluoroethanol to LADH causes a selective quenching of the short-lifetime (Trp-314) component, as has been previously observed by Ross et al. (1981) and Knutson et al. (1982).

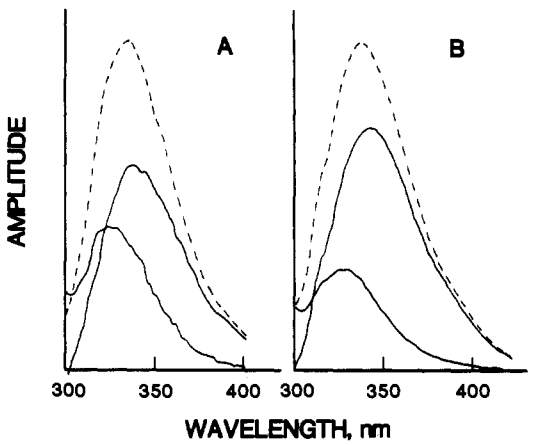

FIGURE 7: Phase-resolved spectra for LADH (A) and the LADH·NAD^+·TFE ternary complex (B). Conditions: 20 °C, excitation at 290 nm, and buffers as given in Table IV.

Table IV: Protein–Ligand Interactions: Fluorescence Lifetime, Iodide Quenching, and Phase-Resolved Spectral Differences[a]

protein	f_1	τ_1 (ns) K_1 (M^{-1}) $\lambda_{max,1}$ (nm)	f_2	τ_2 (ns) K_2 (M^{-1}) $\lambda_{max,2}$ (nm)
LADH (20 °C)	0.439	3.38	0.561	6.74
	0.45	0	0.55	4.6
	0.39	324	0.61	340
LADH·NAD^+·TFE (20 °C)	0.31	1.10	0.69	6.40
	0.38	0	0.62	9.39
	0.27	321	0.73	343
PGK (20 °C)	0.728	0.39	0.272	3.49
		0		0
	0.64	329	0.36	339
PGK·ATP·3-PGA (20 °C)	0.771	0.51	0.229	4.61
		0		0
	0.56	338	0.44	350
metalloprotease (+Ca^{2+}) (10 °C)	0.43	1.20	0.57	5.10
	0.49	0	0.51	4.70
	0.47	318	0.53	350
metalloprotease (−Ca^{2+}) (10 °C)	0.33	1.30	0.67	4.76
	0.27	0	0.73	3.40
	0.34	330	0.66	354

[a] Excitation at 290 nm for lifetime, iodide quenching, and PRS measurements. Fractions (f_i) correspond to the use of a broad bandpass (Corning 7/60) emission filter for the lifetime and quenching studies. The f_i refer to the integrated intensities for the PRS studies. The LADH·NAD^+·TFE complex is formed by the presence of 0.2 mM NAD^+ and 10 mM TFE at pH 7.5 (phosphate buffer). The PGK ternary complex is formed by adding 13 mM 3-phosphoglycerate, 3.2 mM ATP, and 3.2 mM $MgCl_2$ at pH 7.2 (Tris-HCl buffer). The calcium-depleted form of metalloprotease is formed by 10 mM EDTA at pH 9 (Tris buffer).

Discussion

Phase-resolved spectra can be quickly obtained for proteins or other samples, by use of a phase fluorometer at a single modulation frequency. Prior determination of the fluorescence lifetime(s) of the sample is generally needed [see however Keating-Nakamoto et al. (1986)]. PRS measurements are analogous to decay-associated spectral (DAS) measurements but can be made more quickly. Each of the PRS shown here was obtained in 20 min or less.

We show, using a set of two tryptophan containing proteins, that the fluorescence of a protein can be resolved into two components provided that the fluorescence of the protein is a double exponential. We have had little success in trying to resolve three components in a protein with this method.

The proteins we studied each are characterized by a double-exponential decay. Of course, a more complex decay law

will also fit. For example, PGK is probably a triple exponential (Privat et al., 1980). Because each of these proteins has two Trp residues, it is reasonable to expect there to be two decay times. Our PRS show, moreover, that the decay times have distinct associated spectra. In each case, the short-lifetime component is blue shifted with respect to the long-lifetime component. Solute quenching studies confirm the resolution we obtain with PRS for those proteins that can be quenched by iodide.

A major concern regarding PRS measurements with multi-Trp proteins is the possible complications due to excited-state reactions, such as Trp → Trp energy transfer. If such homotransfer occurs, the individual Trp residues will decay in a nonexponential manner. The PRS spectra associated with each decay time will not represent emission solely from an individual Trp residue. As we show in the Appendix, however, characteristic PRS patterns are to be expected when homotransfer occurs, which will enable such excited-state reactions to be identified in some cases.

On comparison of the simulations in the Appendix with the PRS spectra in Figures 3 and 4, it is not clear whether or not energy transfer occurs for most of these proteins. The only case where the PRS strongly indicate energy transfer is in apoazurin Ade when excited at 280 nm. As shown in Figure 4, a characteristic dip below the base line is observed for the short-lifetime component is apoazurin Ade. This negative component corresponds to a negative preamplitude (α) that has been found in only a few proteins by using the pulse/single-photon-counting method (Grinvald & Steinberg, 1974; Petrich et al., 1987). Apoazurin Ade is one of the proteins for which a negative preamplitude has been observed. Petrich et al. (1987) report a negative α for the short fluorescence lifetime of apoazurin Ade, when the pulse–decay pattern is observed at 355 nm. (Because we have a low signal when we attempt to use an emission interference filter or monochromater, together with a Pockels cell modulator, we have not been able to duplicate this result at 355 nm with phase domain measurements. Only by using the Debye–Sears modulator at a single frequency and a larger lamp have we been able to obtain the negative component in the phase-resolved spectrum of apoazurin Ade.) The negative PRS component is more apparent when an excitation wavelength of 280 nm is used, as compared to 290 nm. This is consistent with the "red edge" effect, which is the diminished tendency for concentrated indole solutions to show homotransfer at long excitation wavelengths (Weber, 1960).

The ability to observe the negative amplitude at the long-wavelength side of the short-lifetime component in this protein is due not only to the magnitude of the energy transfer process (k_{ba} in eq A1–A4) but also to the wide separation between the λ_{max} of the blue and red Trp residues. By comparison with the single Trp containing apoazurin from *P. aeruginosa* (Pae), the internal Trp-48 of apoazurin Ade fluoresces with λ_{max} = 308 nm (Petrich et al., 1987; Szabo et al., 1983). This is, of course, an unusually blue Trp residue, and the fluorescence properties of this residue have been much studied and discussed (Finazzi-Agro et al., 1970; Munro et al., 1979; Szabo et al., 1983; Grinvald et al., 1975; Petrich et al., 1987; Turoverov et al., 1985). The surface Trp-118 of apoazurin Ade fluoresces much more to the red, with $\lambda_{max} \approx 350$ nm. Because of this wide spectral separation, the negative amplitude, due to energy transfer from the blue to red Trp residue, can be observed when exciting at 280 nm. The existence of Trp-48 to Trp-118 energy transfer is also indicated by the fact that the fluorescence lifetime of the blue component of apoazurin Ade (τ_1 = 0.75 ns) is much lower than the lifetime of the corresponding Trp residue in apoazurin Pae (τ = 4.2 ns). Assuming that the only source of the additional quenching of Trp-48 in the Ade protein is the energy-transfer mechanism, the rate constant for energy transfer is calculated to be approximately 1×10^9 (transfer efficiency ≈ 80%).

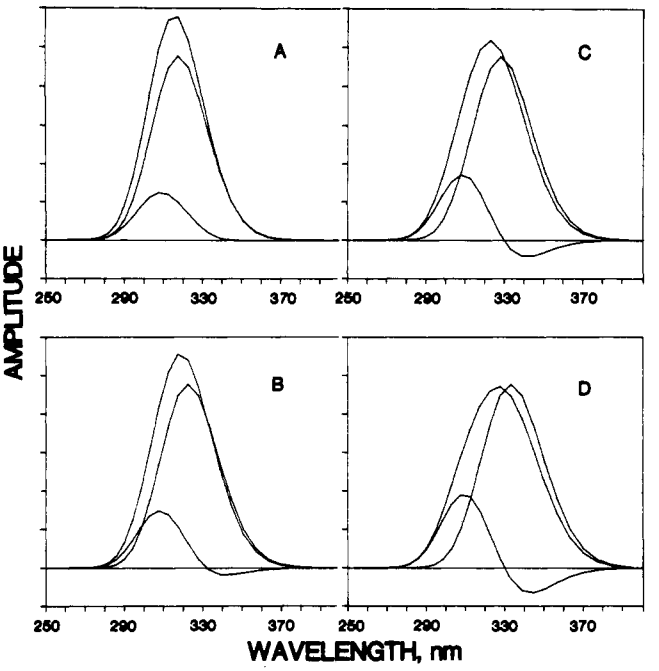

FIGURE 8: Simulated PRS for Scheme I. The top curves are total emission spectra; the subspectra correspond to the emission having $\tau_1 = 1/(k_a + k_{ba})$ and $\tau_2 = 1/k_b$. See eq A1–A5 for explanation. Rate constants used are $k_a = 4 \times 10^8$, $k_b = 3 \times 10^8$, $k_{fa} = k_{fb} = 2 \times 10^8$, $k_{ba} = 1 \times 10^8$, and $\sigma_a = \sigma_b$. For each panel ν_a = 32 kK (=312.5 nm). (A) ν_b = 31.5 kK; (B) ν_b = 31 kK; (C) ν_b = 30.5 kK; (D) ν_b = 30 kK.

No negative component is seen for the other two-Trp proteins studied, but this does not eliminate the possibility of Trp–Trp energy transfer. As shown by the simulations in Figures 7 and 8, if the λ_{max}'s of the two Trp residues are not widely separated, a negative component may not be observed.

Comparison of PRS with solute quenching studies can, however, be used to reveal or discount the existence of such energy transfer. As shown in Figure 8, the steady-state spectral contributions of two fluorescing Trp residues in a protein will be slightly different from the PRS (or DAS) of these residues, when energy transfer occurs. Specifically, the fractional contribution to the steady-state spectrum, at any wavelength, of the donor Trp residue will be larger than the fractional weight of the PRS (or DAS) of the donor Trp, at any wavelength. This is because the amplitude of the short decay time will contain a negative component due to energy transfer [i.e., the amplitude is $\sigma_a C_a(\lambda) - \sigma_a C_b(\lambda)/(k_a + k_{ba} - k_b)$; see eq A3 in the Appendix]. In steady-state measurements, the amplitude for the blue Trp residue is simply given as $\sigma_a C_a(\lambda)$. Likewise, the amplitude, in PRS, of the long decay time will be increased by energy transfer, as compared to the steady-state amplitude of emission from the red Trp residue.

Solute quenching experiments with iodide, or other selective quenchers, can enable the determination of the fractional contribution of individual Trp residues in proteins. If, for example, the fractional contribution (at some wavelength) of the blue (usually least accessible) Trp residue in a two-Trp protein is found to be significantly greater than the fractional weight of the short-lifetime component to the PRS of the protein, this is indicative of an energy-transfer process.

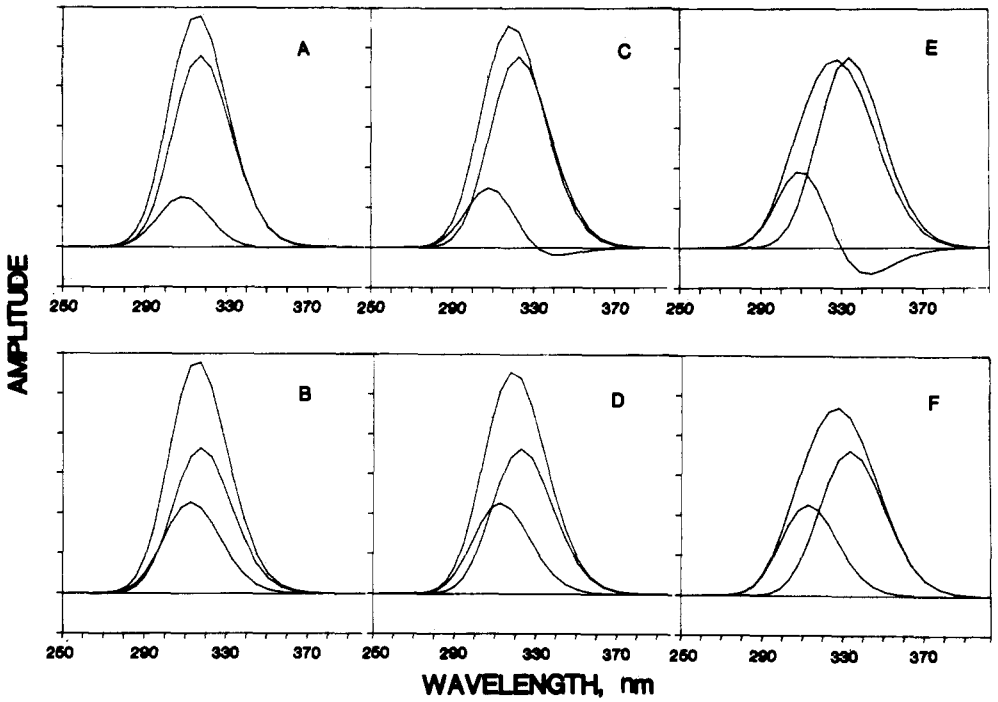

FIGURE 9: Simulated PRS (top) and steady-state component spectra (bottom) for Scheme I. Rate constants $k_a = 4 \times 10^8$, $k_b = 3 \times 10^8$, $k_{fa} = k_{fb} = 2 \times 10^8$, $k_{ba} = 1 \times 10^8$, and $\sigma_a = \sigma_b$. $\nu_a = 32$ kK. For (A) and (B), $\nu_b = 31.5$ kK. For (C) and (D), $\nu_b = 31$ kK. For (E) and (F), $\nu_b = 30$ kK.

Scheme I

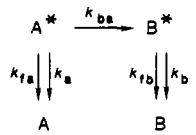

In Table III we give the fractional contributions of the red and blue components from solute quenching experiments with the various two-Trp proteins (using a broad emission filter centered at 350 nm). Likewise, the fractional contributions of the short and long lifetimes, from multifrequency phase/modulation measurements, are given in Table I. In most cases, the fractional contributions of the less accessible and short-lifetime components are in good agreement. From this we conclude that the two Trp residues emit independently in most of these proteins. But for RPK a significant discrepancy is seen. This suggests the existence of energy transfer. (For apoazurin Ade the f_i values in Tables I and III are in reasonable agreement, but recognize that the solute quenching study was performed with excitation at 295 nm, where homotransfer may be limited.)

In summary, the PRS method is a useful method for resolving the component spectra of Trp residues in proteins. This method will enable one to focus on the fluorescence changes that occur in individual Trp residues when, for example, a ligand binds to a protein. If Trp–Trp energy transfer occurs, phase-resolved component spectra will not be simply the spectra of individual Trp residues—recall that PRS (or DAS) give the spectra associated with a particular decay time not necessarily a particular residue. Characteristic negative amplitudes may be observed under favorable conditions of Trp–Trp energy transfer. The comparison of fractional intensities obtained by steady-state solute quenching and lifetime (or PRS or DAS) measurements can give an indication of the existence of such energy transfer. If such an excited-state reaction does not occur, then the PRS will give the spectra of individual Trp residues.

ACKNOWLEDGMENTS

We express our sincere appreciation to Dr. G. E. Norris, Massey University, Palmerston North, New Zealand, and Drs. M. A. Porter and F. C. Hartman, Oak Ridge National Laboratory, Oak Ridge, TN, for generously providing us with protein samples.

APPENDIX

Phase-Resolved Spectra and Effect of Resonance Energy Transfer. Consider the following photophysical model for a protein that contains at least two Trp residues, between which resonance energy transfer can occur. Label the excited states of these residues as A* and B* and consider B* to be a redder emitting Trp residue. This being the case, energy transfer will predominantly be in the direction of A* and B* (i.e., blue to red), with rate constant k_{ba}. Energy transfer in the reverse direction is ignored. Both A* and B* are considered to be populated directly by the excitation source. They will be deactivated by both radiative and nonradiative processes; k_a and k_b are the sum of all deactivation rate constants (except the energy-transfer process), and k_{fa} and k_{fb} are the respective radiative rate constants (see Scheme I). The fluorescence lifetimes $\tau_a = 1/(k_a + k_{ba})$ and $\tau_b = 1/k_b$ characterize the emission decay process, but as seen below, these τ values are not simply assigned to A* and B* due to the kinetic coupling that exists. The individual quantum yields of A* and B* are $\Phi_a = k_{fa}/(k_a + k_{ba})$ and $\Phi_b = k_{fb}/k_b$, and the efficiency of energy transfer is $E = k_{ba}/(k_{ba} + k_a)$.

Following the derivation of similar excited-state rate expressions presented elsewhere (Laws & Brand, 1979), we can express the time and wavelength dependence of the relative intensity of A* and B*, following a Δ function excitation, as

$$I_A(\lambda,t) = \sigma_a C_a(\lambda) k_{fa} \exp[-t(k_a + k_{ba})] \quad \text{(A1)}$$

$$I_B(\lambda,t) = \frac{-\sigma_a C_b(\lambda) k_{fb} k_{ba} \exp[-t(k_a + k_{ba})]}{k_a + k_{ba} - k_b} + \sigma_b C_b(\lambda) k_{fb} + \frac{\sigma_a C_b(\lambda) k_{fb} k_{ba}}{k_a + k_{ba} - k_b} \exp(-t k_b) \quad \text{(A2)}$$

Here, σ_a and σ_b are the normalized, relative absorption coefficients of A and B at the excitation wavelength, such that $\sigma_a + \sigma_b = 1.0$; if $\sigma_a = \sigma_b = 0.5$, there is equal absorption into the two residues. $C_a(\lambda)$ and $C_b(\lambda)$ are the spectral shape and position functions for A* and B*.

The direct, separate observation of decay from A* and B* is not feasible for most cases. One can sometimes monitor the emission at the red emission edge in order to observe primarily B*, but it is technically difficult to achieve selective observation. In general, one observes the decay of the total emission. The following is the impulse/response function for the total emission:

$$I(\lambda,t) = \sigma_a\left[C_a(\lambda)k_{fa} - \frac{C_b(\lambda)k_{fb}k_{ba}}{k_a + k_{ba} - k_b}\right]e^{-t(k_a+k_{ba})} + \sigma_b\left[C_b(\lambda)k_{fb} + \frac{C_b(\lambda)k_{fb}k_{ba}\sigma_a/\sigma_b}{k_a + k_{ba} - k_b}\right]e^{-tk_b} \quad \text{(A3)}$$

$$I(\lambda,t) = \alpha_1(\text{app})e^{-t/\tau_1} + \alpha_2(\text{app})e^{-t/\tau_2} \quad \text{(A4)}$$

As eq A3 indicates, the decay will be biexponential (even if $k_a = k_b$). Note that the apparent preexponential term for the first component, α_1(app), will depend on emission λ, since the difference between $C_a(\lambda)$ and $C_b(\lambda)$ will vary with λ. α_1(app) will be negative if $C_b(\lambda)k_{fb}k_{ba}/(k_a + k_{ba} - k_b) > C_a(\lambda)k_{fa}$, which is likely to be the case at long λ if $C_b(\lambda)$ is redder than $C_a(\lambda)$.

The pertinence of the above impulse–response function to pulse fluorometry is inituitively clear. In phase fluorometry, the exciting light is sinusoidally modulated and the harmonic response that is observed is the Fourier transform of the above type of impulse–response function. As explained in detail elsewhere (Lakowicz, 1983; Jameson et al., 1984), the kinetic parameters (α_i, τ_i) for an impulse–response function can be obtained by analysis of multifrequency phase angle and modulation ratio measurements.

The observed PRS or DAS measurement for such a system will show two subspectra corresponding to τ_1 and τ_2. The first spectrum will be proprotional to $\alpha_1(\text{app})\tau_1$ and the second to $\alpha_2(\text{app})\tau_2$. To simulate such PRS measurements, we will model the spectral shape/position functions for A* and B* as Gaussian distributions [Lakowicz (1983), Chapter X]:

$$C_a(\lambda) = \frac{\exp[(\nu - \nu_a)/\Delta]^2}{2\pi\Delta} \quad \text{(A5)}$$

where ν is wavenumber in kilokaysers (kK) (=1000 cm^{-1}), ν_a and ν_b are the peak positions for A* and B*, respectively, and $\Delta = 2.5$ kK is the width of the distribution [the similar expression for $C_b(\lambda)$ is not shown]. For the blue, donor Trp residue we select $\nu_a = 32$ kK (312.5 nm), and we will allow the position of the red, acceptor residue, ν_b, to range from 32 (319 nm) to 29 kK (344.8 nm).

In Figure 8 we illustrate simulated PRS/DAS spectra for Scheme I where the spectral overlap of the two centers is varied (by changing ν_b). The selected rate constants are $k_a = 4 \times 10^8$, $k_b = 3 \times 10^8$, $k_{fa} = k_{fb} = 2 \times 10^8$, and $k_{ba} = 1 \times 10^8$. The simulation shows that, as the overlap between A* and B* diminishes, a negative amplitude appears for the short decay time at long λ.

In Figure 9 we show similar simulations, and we compare the expected PRS/DAS spectra (top panels) with the steady-state emission that arises from each fluorescing center (bottom panels). That is, the bottom panels give the emission from A* and B* [i.e., for A* we show all the emission with $C_a(\lambda)$, which is $\sigma_a C_a(\lambda)k_{fa}/(k_a + k_{ba})$ from eq A1; likewise, for B* is shown the emission with $C_b(\lambda)$, which is the sum of the preamplitude/decay rates from eq A2].

It is important to distinguish between these PRS/DAS spectra (top) and the steady-state contributions (bottom). The top panels are the spectra associated with either the short or long decay times [i.e., $\alpha_i(\text{app})\tau_i$ in eq A4], and the short decay time will have contributions from emission from both A* and B* (the latter making a contribution with a negative amplitude). The steady-state spectra (bottom) arise from the individual centers, regardless of whether they are populated directly or indirectly. A simple way to realize this is by recognizing that a given excited state, such as B*, does not know how it became excited; it will just fluoresce with distribution $C_b(\lambda)$ and rate constant k_b.

If energy transfer occurs, the PRS/DAS amplitude will usually be less at any wavelength than the corresponding steady-state spectrum for the donor residue, and the PRS/DAS will usually appear larger than the steady-state spectrum for the acceptor residue. Thus the existence of energy transfer should be detected if one can directly compare the amplitudes and shape of PRS/DAS and the steady-state spectra of the components. To obtain the latter is of course the reason PRS/DAS has been developed, so another method is needed. Selective solute quenching can provide an alternate means of determining the fractional, *steady-state* contribution of the two residues (Lehrer, 1971; Eftink & Ghiron, 1976). With eq 2 one can, in favorable situations, determine the fractional contribution of individual Trp residues in proteins. If these fractions are in agreement with the relative fractional contributions at that λ from PRS/DAS measurements, this indicates that the centers emit independently. If these determinations of the fractions do not agree, particularly if the fraction of the short-lifetime component is more in the steady-state quenching than in the PRS/DAS measurement, this indicates the existence of Trp → Trp energy transfer.

Scheme I and the above discussion can be easily extended to model the existence of other excited-state relaxation processes, such as dipole relaxation (Lakowicz & Balter, 1982). If one considers only two excited-state species (i.e., initial and fully relaxed), the impulse–response function will be similar to eq A3, but without the $\sigma_b C_b(\lambda)k_{fb}\exp(-tk_b)$ term since direct excitation into the fully relaxed state will generally not be considered. The simulated PRS/DAS and steady-state subspectra would be similar to those shown in Figures 7 and 8. A multistate relaxation process could also be considered.

References

Anderson, S. R., Brunori, M., & Weber, G. (1970) *Biochemistry 9*, 4723–4729.

Beechem, J., & Brand, L. (1985) *Annu. Rev. Biochem. 54*, 43–71.

Blaszak, J. A., McMillin, D. R., Thornton, A. T., & Tennant, D. L. (1983) *J. Biol. Chem. 258*, 9886–9892.

Brochon, J. C., Wahl, P., & Auchet, J. C. (1974) *Eur. J. Biochem. 41*, 577–583.

Drapeau, G. R. (1978) *J. Bacteriol. 136*, 607–613.

Eftink, M. R., & Ghiron, C. A. (1976) *Biochemistry 15*, 672–680.

Eftink, M. R., & Selvidge, L. A. (1982) *Biochemistry 21*, 117–125.

Eftink, M. R., & Hagaman, K. A. (1985) *Biophys. Chem. 22*, 173–180.

Eftink, M. R., & Hagaman, K. A. (1986) *Biochemistry 25*, 6631–6637.

Eftink, M. R., & Ghiron, C. A. (1987) *Biophys. J. 52*, 467–473.

Eftink, M. R., Wasylewski, Z., & Ghiron, C. A. (1988) Proceedings of the International Symposium on Fluorescent Biomolecules, Bocca di Magra, Italy, Sept 1986 (in press).
Finazzi-Agro, A., Rotilio, G., Avigliano, L., Guerrieri, P., Boffi, V., & Mondovi, B. (1970) *Biochemistry 9*, 2009–2014.
Gratton, E., & Jameson, D. M. (1985) *Anal. Chem. 57*, 1694–1697.
Gratton, E., Limkeman, M., Lakowicz, J. R., Maliwal, B. P., Cherek, H., & Laczko, G. (1984) *Biophys. J. 46*, 479–486.
Grinvald, A., & Steinberg, I. Z. (1974) *Biochemistry 13*, 5170–5178.
Grinvald, A., & Steinberg, I. Z. (1976) *Biochim. Biophys. Acta 427*, 663–678.
Grinvald, A., Schlessinger, J., Pecht, I., & Steinberg, I. Z. (1975) *Biochemistry 14*, 1921–1929.
Hochstrasser, R. M., & Negus, D. K. (1984) *Proc. Natl. Acad. Sci. U.S.A. 81*, 4399–4403.
Irace, G., Balestrieri, C., Parlato, G., Servillo, L., & Colonna, G. (1981) *Biochemistry 20*, 792–799.
Jameson, D. M., Gratton, E., & Hall, R. D. (1984) *Appl. Spectrosc. Rev. 20*, 55–106.
Janes, S. M., Holtom, G., Ascenzi, P., Brunori, M., & Hochstrasser, R. M. (1987) *Biophys. J. 51*, 653–660.
Keating-Nakamoto, S. M., Cherek, H., & Lakowicz, J. R. (1986) *Biophys. Chem. 24*, 79–95.
Knutson, J. R., Walbridge, D. G., & Brand, L. (1982) *Biochemistry 21*, 4671–4679.
Lakowicz, J. R., & Cherek, H. (1981) *J. Biol. Chem. 256*, 6348–6353.
Lakowicz, J. R., & Balter, A. (1982) *Biophys. Chem. 16*, 99–115.
Laws, W. R., & Brand, L. (1979) *J. Phys. Chem. 83*, 795–802.
Lehrer, S. S. (1971) *Biochemistry 10*, 3254–3262.
Longworth, J. W. (1983) in *Time-Resolved Fluorescence Spectroscopy in Biochemistry and Biology* (Cundall, R. B., & Dale, R. E., Eds.) pp 651–728, Plenum, New York.
Petrich, J. W., Longworth, J. W., & Fleming, G. R. (1987) *Biochemistry 26*, 2711–2722.
Privat, J.-P., Wahl, P., & Auchet, J.-C. (1980) *Biophys. Chem. 11*, 239–248.
Ross, J. B. A., Schmidt, C. J., & Brand, L. (1981) *Biochemistry 20*, 4369–4377.
Stryjewski, W., & Wasylewski, Z. (1986) *Eur. J. Biochem. 158*, 547–553.
Szabo, A. G., Stepanik, T. M., Wagner, D. M., & Young, N. M. (1983) *Biophys. J. 41*, 233–244.
Theorell, H., & Åkeson, Å. (1955) *Ann. Acad. Sci. Fenn., Ser. A2 60*, 303.
Turoverov, K. K., Kuznetsova, I. M., & Zaitsev, V. N. (1985) *Biophys. Chem. 23*, 79–89.
Wasylewski, Z., & Eftink, M. R. (1987a) *Eur. J. Biochem. 167*, 513–518.
Wasylewski, Z., & Eftink, M. R. (1987b) *Biochim. Biophys. Acta 915*, 331–341.
Wasylewski, Z., Stryjewski, W., Wasniowska, A., Potempa, J., & Baran, K. (1986) *Biochim. Biophys. Acta 81*, 177–181.
Weber, G. (1960) *Biochem. J. 76*, 335–345.
Weber, G. (1961) *Nature (London) 190*, 27–29.

Characterization of the Internal Initiation of Translation on the Vesicular Stomatitis Virus Phosphoprotein mRNA

Ronald C. Herman*

Virology Laboratory, Wadsworth Center for Laboratories and Research, New York State Department of Health, Albany, New York 12201

Received January 22, 1987; Revised Manuscript Received July 24, 1987

ABSTRACT: Internal initiation of translation on the vesicular stomatitis virus (VSV) phosphoprotein (P) mRNA leads to the synthesis of a second protein [Herman, R. C. (1986) *J. Virol. 58*, 797–804]. Characterization of this phenomenon shows that initiation at the 5′-proximal and internal AUG codons has different optima for mono- and divalent cations in the reticulocyte lysate. Whereas 5′ initiation is stimulated by increasing concentration of K^+ over the endogenous level, internal initiation is inhibited. Internal initiation is much less sensitive to the effects of the cap analogue 7mGpppG in both the reticulocyte lysate and the wheat-germ extract under conditions that reduce 5′-proximal initiation to only about 4–5% of the control level. These results imply that 5′-proximal and internal initiations are distinct biochemical processes.

I recently reported that the 814-nucleotide vesicular stomatitis virus (VSV)[1] phosphoprotein (P) mRNA encodes a second product (M_r 7000; 7K protein) within the 3′ third of the same open reading frame (ORF) encoding the phosphoprotein (Herman, 1986). Translation of this small protein from the capped full-length P mRNA in vitro is specifically initiated at the third of three closely spaced AUG codons (position 623) in both the reticulocyte lysate and the wheat-germ extract (Herman, 1986, and unpublished observations). Initiation at the two in-phase upstream AUGs (positions 512 and 560) is not detected when in vitro or in vivo synthesized P mRNA is

* Address correspondence to this author at Syntex Research, 2375 Charleston Road, Mountain View, CA 94043-1670.

[1] Abbreviations: CBP, cap binding protein; EDTA, ethylenediaminetetraacetic acid; HEPES, *N*-(2-hydroxyethyl)piperazine-*N*′-2-ethanesulfonic acid; M, matrix protein; N, nucleocapsid protein; ORF, open reading frame; P, phosphoprotein; SDS, sodium dodecyl sulfate; SSC, standard saline citrate buffer; VSV, vesicular stomatitis virus; UTP, uridine 5′-triphosphate.

0006-2960/87/0426-8346$01.50/0